Indian Journal of Biochemistry & Biophysics
Vol. 59, March 2022, pp. 296-310

Cryptosporidiosis, a public health challenge: A combined 3D shape-based virtual screening, docking study, and molecular dynamics simulation approach to identify inhibitors with novel scaffolds for the treatment of cryptosporidiosis

Kalpana Katiyar[1]*, Ramesh Kumar Srivastava[2], Ravindra Nath[3] & Gagandeep Singh[4,5]

[1]Department of Biotechnology, Dr. Ambedkar Institute of Technology for Handicapped, Kanpur-208 024, Uttar Pradesh, India

[2]Technology & Business Development Division, Central Institute of Medicinal & Aromatic Plants (CSIR-CIMAP), Lucknow-226 015, Uttar Pradesh, India

[3]University Institute of Engineering & Technology, CSJM University, Kanpur-208 012, Uttar Pradesh, India

[4]Section of Microbiology, Central Ayurveda Research Institute, Jhansi-284 003, Uttar Pradesh, India

[5]Kususma School of Biological Sciences, Indian Institute of Technology, New Delhi-110 016, Delhi, India

Received 08 June 2021; *revised 15 February 2022*

Cryptosporidiosis is a neglected tropical disease caused by the protozoan parasite *Cryptosporidium parvum*. Limited therapeutic options, limitation in *in vitro* parasite culture, and lack of a reliable animal model of parasite for replication of *in vivo* life cycle and drug testing demand alternative methods for drug development. The *in silico* methods of drug discovery prove a crucial process in such conditions.Recent research reported a limited number of small molecules for drug development. Purine nucleotide biosynthesis in *Cryptosporidium* species is dependent on the IMPDH (CpIMPDH) enzyme, so distortion of parasite IMPDH has been pursued as a compelling strategy for curbing *Cryptosporidium* infection due to its different kinetics from the host enzyme. Our study's primary aim was to discover novel ligand molecules with noticeable activity against *Cryptosporidium parvum* IMPDH. For this purpose, we selected 18 previously discovered ligands to understand the interaction feature between ligand and receptor, and their shape and electronic features are employed as a template for shape-based virtual screening of the ZINC database (drug-like subset) search approach via Schrodinger-2019 (Maestro 11.9). The obtained hits were subsequently subjected to structure-based screening, quantum polarized ligand docking (QPLD), and molecular dynamics simulations to fetch potential small molecules with the highest binding affinity for CpIMPDH protein. Further ligand binding energy and pharmacokinetic analysis were also taken into consideration as filtering criteria for selecting the most promising drug-like compounds.

On this experimentation analysis, three top-ranked (ZINC24855054, ZINC58171263, and ZINC08000072) molecules were found to have appropriate pharmacokinetic properties along with surpassing *in silico* inhibitory potential towards the CpIMPDH compared to known inhibitors. The molecular docking and molecular dynamics simulation analysis results satisfactorily confirmed the inhibitory action. Therefore, these new scaffolds deduced by the presented computational methodology could recommend lead molecules for designing promising anti-cryptosporidial drugs targeting CpIMPDH protein.

Keywords: *Cryptosporidium parvum*, Inosine 5′-monophosphate dehydrogenase (IMPDH), MM/GBSA, Molecular Docking, Molecular Dynamics Simulations, Virtual Screening

The novel coronavirus disease 2019 (COVID-19) is one of the most trounced pandemics of the twentieth century who tried to grapple humanity worldwide. COVID-19 is engendered by the severe acute respiratory syndrome coronavirus 2 (SARS-CoV-2). The rapid transmission drive of SARS-CoV-2, high mortality and morbidity, and unavailability of treatment options are chief factors responsible for the pandemic dispersal. The COVID-19 has conquered the year's headlines and geared all significant research attention. The everyday cost of common parasitic diseases has been disoriented under the shadow of COVID-19. The parasitic diseases are considered as a considerable reckoning on local communities. Hitherto, because most of these parasitic diseases are no longer endemic to developed nations, the projects underlying research and development of parasitic diseases are not funded at levels that are proportional to their global morbidity and mortality. The scientific and public health communities' energy and attention concern the COVID-19, but though managing this, it

*Correspondence:
E-mail: kalpna@aith.ac.in

will be essential to show steadfast resolution toward interpretation and combating the parasitic diseases[1]. The COVID-19 pandemic has turned the clock back by years in the fight against other parasitic diseases, and it has interrupted research, trials, and other efforts to ease the public health burden.

Tyzzer first recognized *Cryptosporidium* species (spp.) in 1907, but it remained undercover until the 1980s when AIDS became endemic in humans. The parasitic possessions are considered primary etiological agents responsible for various clinical complications associated with gastrointestinal epithelium among infants and immunocompromised persons. Specific medical and symptomatic complications led by *Cryptosporidium* spp. infection include watery diarrhea, nausea, fever, and in extreme cases, neuro-development disorders. Such medical situations are categorized as cryptosporidiosis disease[2]. The cryptosporidiosis disease burden varies geographically. A recent systematic review on epidemiological analysis of human *Cryptosporidium* infection in China (1987-2018) asseverated average prevalence of *Cryptosporidium* was 2.97% in reported areas. Among these, 1.77-12.87%infection prevalence is found in rural areas compared to 0-3.70% prevalence in urban areas. The nationwide prevalence of *Cryptosporidium* in humans is 0.1-14.1% in Asian countries,2.6-21.3% in African countries,0.1-14.1% in Europe,3.2-31.5% in central and south American countries, and 0.3-4.3% in North America[3]. A meta-analysis study on the prevalence of the *Cryptosporidium* in HIV-positive patients reported 11.2% prevalence and 14.4%globally. The low number of$CD4^+$ cells in AIDS patients is one primary reason for the high infection rate[4]. The most prominent epidemiological studies like MAL-ED (Etiology, Risk Factors, and Interactions of Enteric Infections and Malnutrition and the Consequences for child health and development), GEMS (Global Enteric Multicenter Study), and GBD (Global Burden of Disease) reported that *Cryptosporidium* spp. was among the most critical pathogens for diarrheal infections in children under 12-month-old and community clinics. The *Cryptosporidium parvum* (*C. parvum*) infection is associated with a long duration of diarrhea and 2-3 fold higher mortality rates in malnourished young children than healthy ones[5]. *Cryptosporidium* spp. induced pediatric diarrhea accounts for 9% of global child mortality and 50% of water-borne infections in the United States due to *Cryptosporidium*[6]. The primary infectious species of the parasite associated with human and animal infections are *C. parvum*, *C. hominis*, *C. meleagridis*, *C. andersoni*, *C. felis*, *C. suis*, and *C. canis*. However, more than 39 species and 30 genotypes of *Cryptosporidium* spp. are identified *C. parvum* and *C. hominis* are associated with 90% of cases of human infection. The small subunit (SSU) rRNA gene and glycoprotein 60 (gp60) gene are validated genetic markers for phylogenomic analysis of the parasite. The genome identity between *C. hominis* and *C. parvum* lowa II is 96.85%. The subtle variation in the genome of *C. homins* and *C. parvum* are responsible for phenotypic differences in host-parasite interface proteins[7]. The parasite stuck a monogenous life cycle with both the asexual and sexual phases. The life cycle begins with the ingestion of sporulated oocysts. The oocysts are resistant to the environment and generalized sterilization methods. After ingestion, oocyst excystation occurs in the upper intestine releasing four sporozoites. The sporozoites penetrate nearby intestinal epithelium cells and settle in the parasitophorous vacuole. It is intracellular but extra-cytoplasmic.A feeder organelle made a channel between the parasitophorous vacuole and host cell cytoplasm.

From 2004 up to the recent five-year period, scientists have failed to design a fully effective therapeutic agent to resist parasite invasion. Parasite contaminated dietary and other products act as a way forward for its transmission to reach the gastrointestinal tract, where the parasite utilizes host cellular metabolites via pedestal and feeder organelle[8].

Taxonomically, *C. parvum* (genome size approx 9 Mbp), *C. hominis*, and *C. fragile* are placed in the same Phylum (Apicomplexa) as *Plasmodium* spp. and *Toxoplasma* spp. Intriguingly, in comparison to *Plasmodium* spp. and *Toxoplasma* spp. significant gene loss was reported in *C. parvum* encoding 3,500 genes[9]. Metabolic interventions following *C. Parvum* synthetic machinery apicoplast and mitochondrial genome loss proved insufficient to overcome parasite pathogenicity[9]. Parasite persistent pathogenicity indicates the existing knowledge gap to understand unexpressed glycolytic enzymes responsible for the unusual microbial energy generation mechanism[10].

Similarly, *C. parvum's* intracellular metabolic mechanism matched obligate parasites like *Rickettsia* spp. and *Chlamydia* spp, which command over host synthetic machinery for survival. Parasite's unique anabolic mechanism indicates possible therapeutic targets to inhibit parasitic growth[11]. Following CRISPR/Cas9, a gene disruption technology, scientists unveiled Dihydrofolate Reductase-Thymidylate Synthase (DHFR-TS) and Inosine Monophosphate

Dehydrogenase (IMPDH) enzymes as a suitable target for drug designing to overcome *C. Parvum* pathogenicity. Both enzymes are integral in marinating parasite energy via importing host purines[12]. Targeting IMPDH and DHFR-TS enzymes with specific drug molecules were of great importance to inhibit the parasitic life cycle[1314]. Scientific efforts regarding drug designing and Nitazoxanide's discovery, Paromomycin made significant contributions regulating *C. parvum* growth among infants and adults with the compromised immune system. However, it failed to kill *C. parvum* completely. The underlying reason for the in effectiveness of Nitazoxanide and Paromomycin is still debatable[15,16]. Recent progress made by scientists identifying IMPDH structural characteristics, inhibition, potent inhibitors' selection, and potential lead molecules' identification indicated encouraging results over the model organisms. *C. parvum* IMPDH (CpIMPDH) protein has distinct genomic and structural characteristics compared to mammalian IMPDHs[17].

Cryptosporidium parvum lacks adenine and guanine synthesis; as usual, most parasite siblings synthesize and relyupon the host nucleosides *via*the CpIMPDH pathway to convert IMP (inosine 5′-monophosphate) into xanthosine 5′-monophosphate[18]. Medical applications of benzoxaborole derivatives activity inhibiting aminoacyl-tRNA synthetases activity during fungal and bacterial protein synthesis led to the development of FDA-approved effective therapeutic ligands against gram-negative bacteria[19]. However, the development of effective therapeutic molecules against CpIMPDH is questionable after significant scientific progress.

Virtual screening is an essential aspect of the modern drug discovery process. It reduces resources, cost, and overall time in the drug development process. It also dispenses novel chemical species with desirable activities from diverse chemical databases. The output of virtual screening candidates has been proven to be an appropriate starting point for further exploration and development in the drug discovery process. The ligand and structure-based virtual screening are routinely practiced in most successful drug discovery projects[20]. Despite much research in the last decades, only a few inhibitors against CpIMPDH with good pharmacokinetic properties have been uncovered. Thus, there is room to develop novel and potent chemotypes or optimize existing inhibitors against CpIMPDH to curb *Cryptosporidiosis*.

Structure-less ligand prioritization approaches were followed by many scientists covering minimal future drug development aspects treating Cryptosporidiosis. Molecular modeling prioritizing existing ligand molecules via computational analytical tools, including virtual screening and ligand enzyme structure-activity relationship, seems revolutionary for drug discovery and development. While prioritizing ligand molecules based on enzyme-ligand compatible molecular characteristics in the availability of thousands of an average efficacy ligand, it seems an excellent challenge for pharmacologists to shortlist the most effective ligand molecule against *Cryptosporidium*[21].

Currently, molecular dynamics is the best available protein-ligand interaction approach to cross high energy barriers within the feasible time duration to achieve protein-ligand interaction at unusual temperatures[22]. Molecular dynamics calculations from multiple ligand positions are routinely adopted to estimate protein-ligand compatibility and energy gap minimization[23]. Ranking and evaluating ligand domains and predicting binding domains is vital for the virtual screening structure[24]. Calculation of reliable protein-ligand complexes scoring requires excellent expertise to distinguish between active and inactive protein-ligand complexes[25].

About retrospective therapeutic challenges, our study aims to discover amino-methyl benzoxaborole based novel ligand molecules with visible activity against *Cryptosporidium parvum.* At the same time, the significant objectives include standardization of treatment strategies following Cryptosporidiosis, virtual screening of potential ligand molecules, comparative structural activity relationship, preparation of 3D ligand molecules, and identification of effective therapeutic agents among immune-compromised patients.

This work predicted the 3D structure of the inosine monophosphate dehydrogenase receptor from its amino acid sequence deploying various tools. The 3D structure was predicted using a threading approach that relies on the observation that all naturally occurring proteins have limited fold, so relatively distant homologous proteins have a similar structure, and predicted 3D model quality is checked thoroughly at various levels.

The present investigation aims to identify novel inhibitors of *C. parvum* IMPDH enzyme using a combination of various *in silico* approaches like

shape-based screening (SBS), ADMET, molecular docking, and molecular dynamics studies. The present study can be used as a pilot for the rational drug design for other pathogenic microbes and cancer treatment.

Materials and Methods

Hardware and software specifications

In this study, Schrodinger's Drug Discovery Suite 2015 (evaluation/trial version)with Module Maestro 11.9, Shape Screening Module, Merge Duplicates Module, Virtual screening workflow Module, Protein Preparation Wizard Module, LigPrep Module, QikProp Module, Prime/MM-GBSA Module installed on Intel® core(TM) i3-8100 CPU @3.60 GHz,64 GB RAM with a 2GB graphics card exploited for all computations in this research.

Shape-based molecular similarity screening

The shape-based molecular similarity is a new strategy for discovering new chemical scaffolds. It relies on the principle that if two molecules are structurally similar, they frequently have a similar biological function and physical properties. This similarity approach is an advanced tool for the virtual screening of an extensive database of compounds. Molecular similarity analysis between two molecules can be performed through (i) structural representations and (ii) quantitative similarity measurement among the two entities.

We followed the shape screening approach via Schrodinger-2019 (Maestro 11.9), a molecular shape screening computational tool [26]. Similarly, pharmacophore models, also called quantitative 3D tools for novel inhibitor validation tools, were also used in virtual screening protocols[27]. Before following quantitative pharmacophore modeling analysis, the feature mapping module was adopted for each presented molecule. The primary aim was to shortlist the universal potent ligand molecule. Outcomes in terms of hydrogen bond acceptor, hydrogen bond donor, hydrophobic, and aromatic ring ligands were effectively mapped with molecules under consideration, and calculated features were considered to generate hypotheses and identify potential ligands. Simultaneously, uncertainty in the pharmacophore model was the critical parameter to care about while determining agonist. The preferred value set for uncertainty was about a 2-3 magnitude level[28]. The ZINC database (drug-like subset) is a free, commercial database of over 10 million purchasable compounds supported by the Department of Pharmaceutical Chemistry at the University of California, San Francisco(UCSF)[29].The 3D structures of 18 previously reported CpIMPDH inhibitors were taken on board to find similar drug-like compounds with a threshold limit of 80% similarity. The output of 2000 hitswas saved in a suitable file format.

Before proceeding towards the structure-based virtual screening (VS), ligand preparation is essential for generating three-dimensional (3D) geometries, bond order correction, and generation of accurate tautomer and ionization steps. LigPrep module generates the most appropriate ionization state (pH=7.0) for each ligand molecule. The OPLS-AA_2005 force field was used to generate the lowest energy conformers of ligands[30].

Toxicity and ADME studies

It is desirable that candidate ligand molecules passed through VS protocol must have good ADMET profiles. Nowadays, various *in silico* tools are available to investigate the pharmacokinetics, toxicity, bioavailability, and safety. QikProp (rapid ADME predictions of drug candidates) module in Schrodinger drug discovery suite was used to predict MDCK and Caco-2 cell permeability, overall CNS activity, octanol/water, and water/gas log Ps, log S, and log BB like pharmaceutically relevant properties[31].

Target protein preparation

The primary structure of the target protein sequence (Accession number AF426177) was retrieved from GeneBank (https://www.ncbi.nlm.nih.gov/genbank/)[32]. The homolog structure was identified through BLAST using the PDB database. The highest homology was pragmatic (PDB ID:4IXH), having 95% similarity with 95% query coverage. The enzyme structure (PDB ID:4IXH) was chosen for the reference receptor protein structure. It is the catalytic domain crystal structure of CpIMPDH (resolution- 2.105 Ă) with (2S)-2-(naphthalen-1-yloxy)-N-[2-(pyridin-4-yl)-1,3-benzoxazol-5-yl] propenamide inhibitor along with substrate submitted in protein data bank **(**https://www.rcsb.org/)[33]**.**

The successful outcome of molecular docking protocol relies on the optimized three-dimensional (3D) structure of protein and ligand for the precise binding affinity prediction. Therefore, the modeled 3D structure of the protein is evaluated for any structural quality distortion. The central aspect is to scrutinize unusual conformation, residue packing

anomaly, sequence-structure mapping, residue-shift error, and errors due to incorrect side-chain residue. The PROCHECK tool was deployed for structure validation of the protein[34].

Receptor protein was prepared using the protein preparation wizard by involving the parameters like assigning bond orders to hydrogen's, zero-order bonds created to metal atoms, creating disulfide bonds, and de-solvation out by deleting the crystallized free water molecules beyond 5Å[30].The protein 3D structure integrity was checked, and appropriate modification was done. The tautomeric and protonation states of Glu, Arg, His, Lys, and Asp were adjusted, and also the orientation of Gln and Asn residues generated. Finally, the protein hydrogen bonds were optimized and minimized using the force field OPLS3e[35]. With the receptor generation program from the Glide module, the active pocket in the protein was fixed for docking[36].

Structure-based virtual screening

The hits (1595) retrieved through the similarity search approach were passed through the structure-based virtual screening module against the active- site of the prepared CpIMPDH target protein. It is a multi-step screening procedure with Lipinski's Rule of 5 (ROS) and reactive group filter placed at the appropriate position to remove hits with chemically active functional groups and undesirable drug-likeness properties. The extracted hits were passed through docking by Glide docking protocol which consists of High-throughput Virtual screening (HTVS), Standard Precision (SP) , Extra Precision (XP) anddocking protocol. Docking calculations were first performed in HTVS mode, and the top 50% best-docked hits (999 compounds) were passed through the subsequent SP docking calculations. Finally, the top 30% (299 compounds) of the SP docking protocol were passed through the XP docking screening protocol. XP Glide scores were used to sort the best-docked ligands[36,37].

Most of the docking protocols are molecular mathematical calculations in which the polarization effect of a ligand is not considered. It is now well characterized that the electrostatic charge on molecules has a paramount role in ligand-receptor protein interaction in docking. As a result, in order to reduce the false positive hits, QPLD protocols were applied to the screened compounds from the previous filter. In the QPLD protocol, the ligand atoms are contemplated at the quantum mechanical level. In the execution of this protocol same grid-level parameters were used that had already been set in virtual screening docking calculations[38]. Docking calculations were carried out in two steps, initially Glide Standard precision protocol (SP) docking protocol. In the subsequent step, the protein field-induced polarization effect on ligands was calculated which is conjoined with Jaguar quantum mechanics. Density Functional Theory (DFT) method was applied in scoring ligands docked in target protein and elucidated by the OPLS-2005 force field. In the end, ligands were strained based on lower values of XP Glide Score and interacting amino acid residues[39,40].

To further enhance the virtual screening protocol's productivity and remove the pitfall of the scoring function of Glide Score, the best ligand-protein complex picked from QPLD studies was subjected to an MM-GBSA analysis[41].It prioritized ligands based on the relative binding free energy Δ (G)between ligand and receptor molecule.

$$\Delta Gbind = G\ complex - (G\ protein + G\ ligand)$$
$$= \Delta EMM + \Delta GSOL$$
$$\Delta GSOL = \Delta GGB + \Delta GSA$$

Where: ΔEMM-minimized energy difference between protein-ligand complex and the total energy of protein and unbound ligand, ΔGSOL-solvation free energy difference obtained by the polar (ΔGGB) and non-polar (ΔGSA) solvation energy.

Molecular dynamics simulation

The best-ranked ligands from the MM-GBSA study were further scrutinized in molecular dynamics simulation protocol to evaluate ligand stability of binding mode and thermodynamic performance in the receptor protein (CpIMPDH) active –site[42]. Molecular dynamics (MD) simulation of docked complexes was done byGROMACS package 5.1 to unveil the docked ligands' structural behavior[43]. The simulation was done using a GROMOS 43a1 force field and systems solvation by using a water model, single point charge (SPC) cubic box apart 1.0 nm from the surface of the protein box. Both systems were neutralized by their corresponding ions. The existing energy gap in docked complexes was processed *via* the steepest descent algorithm by following about 50,000 steps used for each simulation to meet the complex's stability.

Similarly, equilibration of both systems was achieved by using NVT and NPT ensembles for 100ps each. The V-rescale thermostat was used for equilibration with a reference temperature of 310.15 K

for 1 ns. Finally, the production MD run was performed with 100 ns time duration. GROMACS in-built tools were used to compute protein RMSD and RMSF[44,45].

Results and Discussion

This study's main objective is to identify novel and promising lead molecules that interfere with CpIMPDH and are deployed as potential anti-cryptosporidial agents. An integrative and highly superior virtual screening protocol incorporating various *in silico* approaches (shape-based virtual screening) is deployed in a stepwise riddler approach to fulfill this objective. Beneath the result of various computational approaches applied for the efficient identification of inhibitors against CpIMPDH are presented and discussed.

Target protein preparation and binding mode analysis

The Protein preparation wizard was used for receptor protein preparation by polar hydrogen atom addition, crystallographic water molecule removal, disulfide bond creation, missing side chains, and loops correction. The parameters like assigning bond orders to hydrogen, zero-order bonds creation to metal atoms, creating disulfide bonds, and de-solvation were carried out by deleting the crystallized free water molecules beyond 5Å. The protein 3D structure integrity was checked, and appropriate modification was done. The tautomeric and protonation states of Glu, Arg, His, Lys, and Asp were adjusted, and also the orientation of Gln and Asn residues generated. Finally, the protein hydrogen bonds were optimized and minimized using the force field OPLS3. With the receptor generation program from the Glide module, the active pocket in the protein was fixed for docking. The coordinates of the co-factor NADH were transferred into the enzyme structure at its binding domain, and the coordination pose was compared with other reported structures of CpIMPDH. In the native conformation of the protein, each atom is in equilibrium and thermal stable, but as temperature increases or protein interacts with the ligand or solvent creates oscillation of atom around the equilibrium position. The B-factor profile of an atom in a protein describes the displacement of the atom from the lowest energy or equilibrium position. For this receptor protein, a normalized B-factor graph is shown in (Fig. 1). It is in the permissible range as most of the amino acid residues havea negative value that indicates a more stable position of that residue.

Furthermore, protein is also checked for any atomic disorder. For this, a plot of the probability of disorder (on the y-axis) for each numbered residue (on the x-axis) is generated. All the residues above the threshold (shown as a dashed line on the plot) could be considered disordered and below as mostly ordered and shown in (Fig. 2).

Again OPLS-2005 force field was used for energy minimization of receptor protein with RMSD cut-off up to 0.90 Å. The receptor grid box was generated around the center of the receptor protein active site with a cubic volume of 50 × 50 ×50 $Å^3$ with a grid point spacing of 0 .974 Å. The induced-fit docking protocol was employed, the maximum number of energy evaluations was set as 20,00,000 per run.

Shape-based molecular similarity screening

Huston CD *et al*, 2015 performed a structure-activity relationship (SAR) testing benzimidazole activity against *C. parvum* IMPDH and explained its significant possibility as a potential inhibitor to overcome Cryptosporidiosis. Another similar SAR-based study focusing on phthalazine reported benzofuranamide derivatives' role in inhibiting minute concentration of *C. parvum* IMPDH protein. They

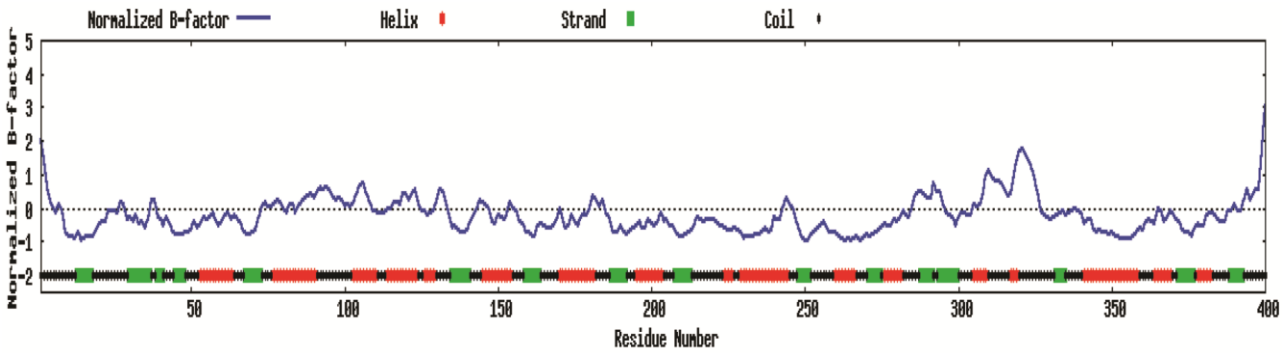

Fig. 1 — The normalized B-factor graph of receptor protein showing each amino acid residues' stability in native conformation

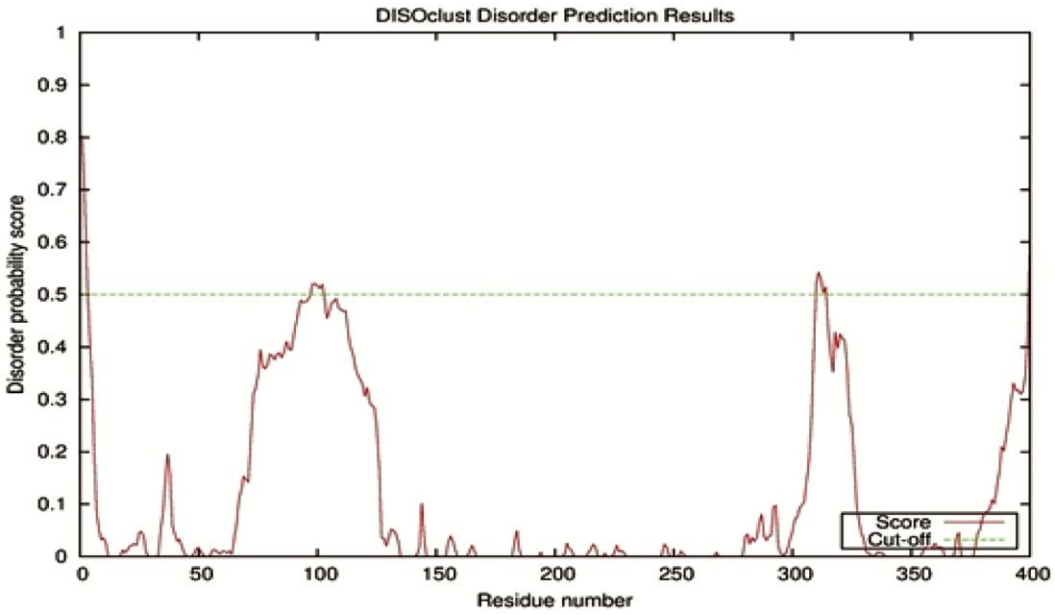

Fig. 2 — A plot of the probability of disorder (on the y-axis) for each numbered residue (on the x-axis) of the receptor protein

highlighted that these scaffolds have an impact on inhibiting CpIMPDH activity. While another approach led by Teotia *et al*, 2018 screening 38 benzoxazole derivatives docking four compounds revealed adverse outcomes over the model organisms. The most competent outcome introducing heterophilic pyridine substituents at benzoxazole 2-position highlighted enhanced CpIMPDH inhibitory action with super antiparasitic sensitivity. Literature reported 4-oxo-benzopyrano[4,3-c] pyrazole derivative in literature as an average potent inhibitor following CpIMPDH in comparison to urea-based selective inhibitors with leading potency and stability[46,47]. To extract all essential features of previously designed active ligands, the most active representatives of benzoxazole series, phthalazinone derivative series, and urea-based inhibitor series were used for shape-based screening (SBS) in order to screen the database and shown in (Fig. 3). The 3D shape-based screening was run with default parameters, search type pharmacophore types, and the maximum number of conformers was set as 100. This analysis was performed by overlaying and superpositioning of generated conformer in a way that allows maximum volume overlap. The underlying algorithm calculates atomic overlap mathematically. Approximately 1800 new molecules were identified. Following its merge module, 1500 duplicate records were removed with the identification of 18 *Cryptosporidium parvum* IMPDH potential inhibitors, as shown in (Fig. 3A). These 18 ligandsCpIMPDH inhibitor molecules were selected as a training ligand data set for a similarity search in a ligand-based virtual screening experiment. The ZINC database was screened for retrieving compounds with 80% structural similarity concerning the training ligand set dataset, and VS workflow is shown in (Fig. 4).

Merged 1595 ligand molecules were tested and prepared by the LigPrep module. After ligand preparation, 488 new conformations of ligands were generated. The 2D structures of all ligands were converted to 3D using LigPrep using the default settings. According to the user manual, (i) hydrogens were added, (ii) salts were removed, (iii) stereoisomers were generated, (iv) probable ionization states were calculated at pH value of 7.0 ± 2.0 using the module specified chirality was retained, and energy minimization of each structure was carried out using OPLS3e force field. Lipinski's filter-based rule of five, a standard criterion for differentiating compounds from drug molecules including MW< 500, Partition coefficient log P<5, donor HB< 5, acceptor HB <10, was applied to focus all ligands, only 1999 ligands passed Lipinski's rules.These 2083 ligands' ADME properties were calculated by the QikProp module.

Molecular docking studies

QPLD docking studies were performed for 2000 compounds having satisfactory predicted activities for the best binding confirmation into the active site of

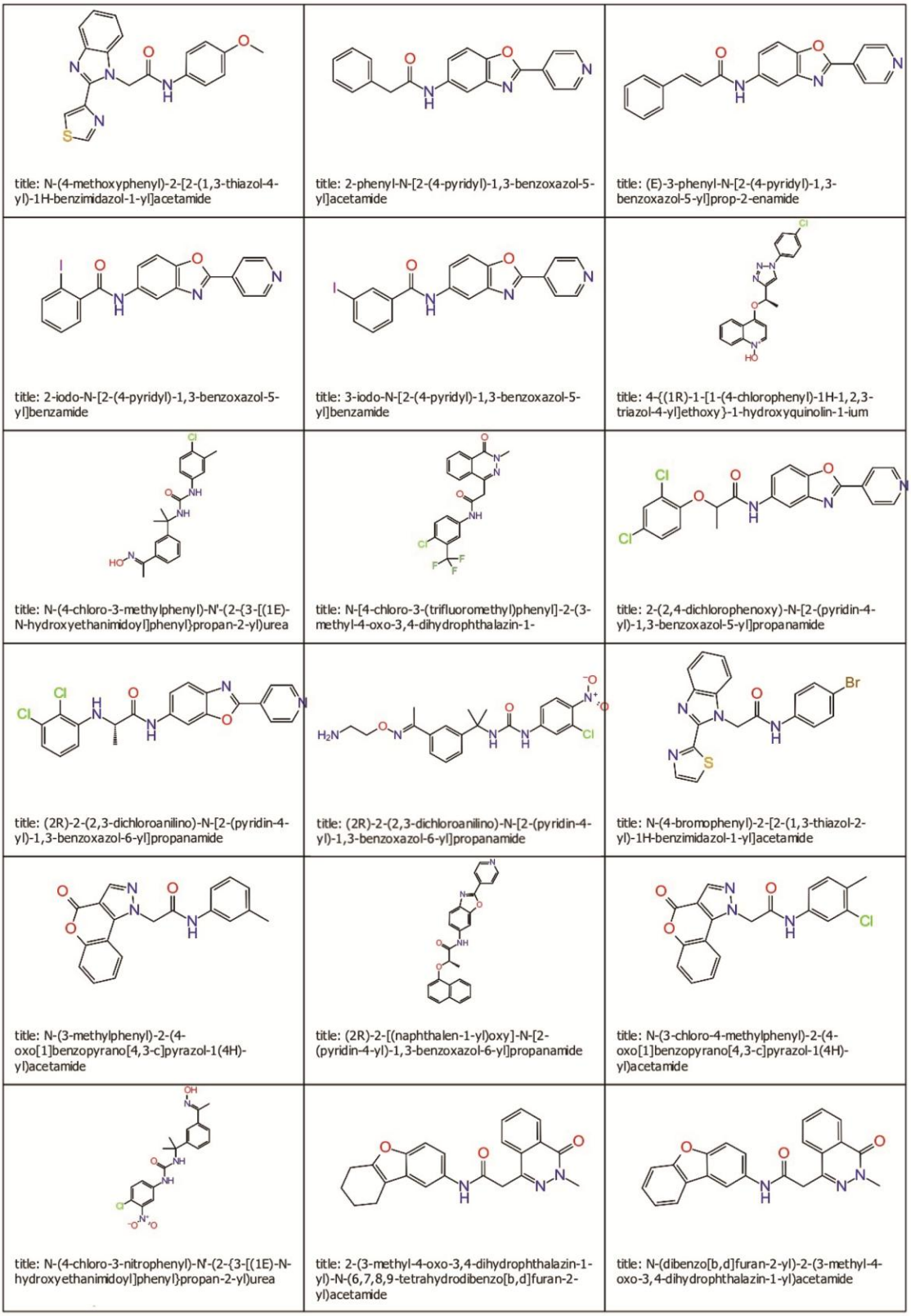

Fig. 3 — The benzoxazole series, phthalazinone derivative series, and urea-based inhibitor series ligands molecules deployed for shape-based screeningprocess implemented in this study

CpIMPDH, subjected to QPLD molecular docking studies[42]. The crystal structure of CpIMPDH (PDB ID: 4IXH) after relevant modifications was exploited for docking calculations. Phthalazinone and Benzimidazole were docked as a reference compound to validate docking protocol. A flow diagram of the molecular docking process employed in this study is shown in (Fig. 5).

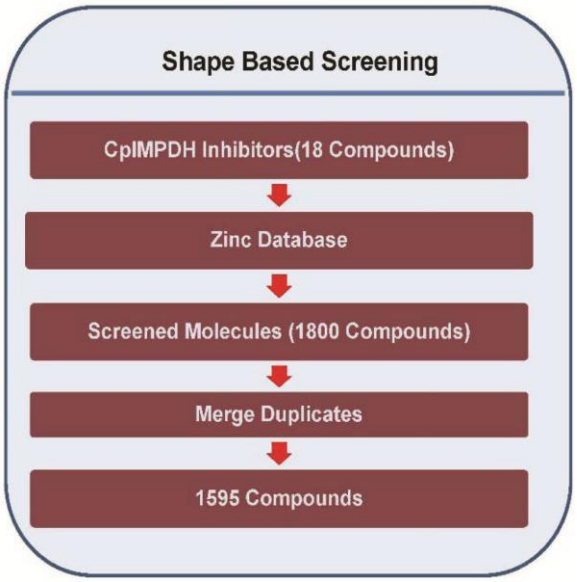

Fig. 4 — Schematic representation of the shape-based screening

The biologically active form of CpIMPDH exists as a tetramer, and each monomer consists of 400 amino acid residues. The residues Ser48, Ser217, SER276, Gly303, Met302, Tyr299, Gly275, Asp252, and Gly254of each chain are active sites and located near the interface region. Among these are mobile catalytic strings (residues 302-330) to help cofactor detachment during the enzymatic reaction. IMPDH catalyzed reaction completes in two-phase. In the first phase, catalytic Cys219 makes a nucleophilic attack on the IMP and forms a covalent intermediate E-XMP* (transition state) and NADH. In the second phase, mobile catalytic Cys residue and a putative water molecule hydrolyze E-XMP* to Enzyme and XMP.

Literature survey revealed that previously discovered CpIMPDH inhibitors consist of two aromatic moieties. One aromatic ring makes π-stacking interactions with the purine base of IMP while the other aromatic ring interacts with adjacent chain Tyr358 amino acid residue. This interaction changes the inhibitor's conformation and allows the formation of a hydrogen bond with Glu329 amino acid residue.

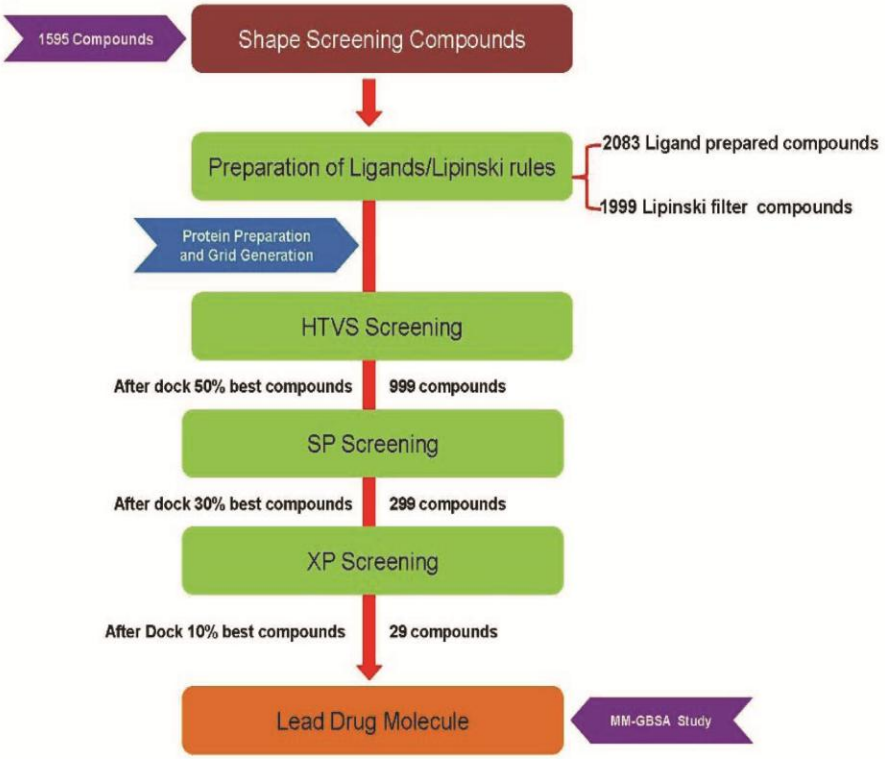

Fig. 5 — Schematic representation of the molecular docking process employed for structure-based virtual screening

The 1999 ligands with satisfactory docking scores from the first phase of docking carried out to filter similar compounds from the ZINC database were subjected to QPLD calculations for a more accurate determination of binding mode. Reference compound docking score (−6.174 to −7.768 Kcal/mol) was used as filtering criteria, and compounds having lower docking scores were ranked based on the XP Glide score.

The Molecular Mechanics and Poisson-Boltzmann or Generalized Born and Surface area continuum Solvation (MM-GBSA) post docking calculations have been performed to the best-docked pose of each ligand. The MM-GBSA estimates binding free energy between molecules based on electrostatic, vander Waals interactions, polar solvation, and non-polar solvation energy. The final rankings of the ligands were carried out based on the obtained free energy of binding (ΔG_{bind}). All the ligands having lower free energy (against reference ligands) were arranged in decreasing order of free binding energy.

A total of 29 ligand molecules flaunted acceptable binding free energies (ΔG_{bind}) together with prerequisites non-covalent bonding interactions with active siteGly275, Ser276, and ser217 residues shown in (Table 1).

The selected ligands have shown lower binding free-energy values than known inhibitors docked to the same pocket of CpIMPDH. Moreover, the detailed inspection of docking results has revealed that the van der Waals (Glide evdw (Kcal/mol) and the Coulomb energy (Glide ecoul (Kcal/mol)) are the most critical energy determinant contributing towards ligands binding energy. Among the 29 ligands, three ligands (ZINC 24855054, ZINC 58171263, and ZINC08000072) molecules have −7.764 kcal/mol, −7.752 Kcal/mol, and −7.438 Kcal/mol. The XP glide score was (−80.944) Kcal/mol, (−83.157)

Table 1 — Binding energy result of the finally selected compounds from the ZINC database screened by successive shape-based screening, ADMET filter, and Molecular docking filter

S.No.	Ligand ID	SP Glide Score Binding Energy (Kcal/mol)	XP Glide Score Binding Energy (Kcal/mol)	ΔGSolGB (Kcal/mol)	ΔGvdW (Kcal/mol)	ΔGcoulomb (Kcal/mol)	ΔGLipo (Kcal/mol)	ΔGcovalent (Kcal/mol)	ΔGHbond (Kcal/mol)	ΔGbind (Kcal/mol)
1	ZINC24855054	−7.764	−7.768	−7.768	−48.229	−7.382	−55.611	6.706	−1.745	−86.543
2	ZINC58171263	−7.752	−7.752	−7.752	−42.296	−11.548	−53.844	0.527	−1.57	−85.046
3	ZINC08000072	−7.438	−7.438	−7.438	−34.293	−7.252	−41.545	0.645	−0.403	−83.157
4	ZINC71375394	−7.413	−7.413	−7.413	−52.565	−5.663	−58.229	3.647	−0.35	−82.166
5	ZINC00205921	−7.335	−7.336	−7.336	−50.034	−5.998	−56.031	2.304	−1.143	−81.835
6	ZINC44685020	−6.941	−6.941	−6.941	−40.636	−10.363	−50.999	−1.934	0	−81.756
7	ZINC44192084	−6.874	−6.874	−6.874	−41.849	−6.969	−48.818	5.3	−0.469	−80.944
8	ZINC14200809	−6.784	−6.784	−6.784	−45.882	−6.808	−52.691	3.132	−1.33	−78.413
9	ZINC02978189	−6.762	−6.762	−6.762	−40.656	−8.596	−49.252	11.975	−1.544	−77.252
10	ZINC86189966	−6.749	−6.749	−6.749	−39.461	−8.547	−48.008	1.648	−1.4	−76.763
11	ZINC75162825	−6.724	−6.724	−6.724	−37.535	−10.712	−48.247	2.781	−0.762	−75.073
12	ZINC77878093	−6.602	−6.669	−6.669	−42.469	−6.276	−48.745	4.306	−0.7	−74.636
13	ZINC58417699	−6.597	−6.637	−6.637	−38.698	−3.631	−42.329	4.434	−0.175	−73.886
14	ZINC79689858	−6.624	−6.624	−6.624	−46.827	−9.797	−56.624	1.639	−1.208	−73.586
15	ZINC03608608	−6.594	−6.594	−6.594	−38.693	−8.919	−47.612	3.552	−0.156	−73.027
16	ZINC12539837	−6.576	−6.581	−6.581	−48.866	−7.407	−56.274	−7.574	−0.351	−72.883
17	ZINC63450248	−6.532	−6.532	−6.532	−45.412	−6.093	−51.506	0	0	−71.776
18	ZINC75162691	−6.518	−6.518	−6.518	−38.52	−9.565	−48.085	1.885	−0.425	−70.225
19	ZINC45755764	−6.51	−6.51	−6.51	−43.956	−8.503	−52.458	4.304	−0.908	−69.799
20	ZINC79689842	−6.483	−6.483	−6.483	−46.011	−8.78	−54.792	0.991	−1.17	−69.606
21	ZINC79689787	−6.421	−6.421	−6.421	−47.04	−10.071	−57.111	5.019	−1.166	−69.176
22	ZINC38550569	−6.345	−6.377	−6.377	−41.745	−7.904	−49.648	5.148	−0.791	−67.744
23	ZINC40307723	−6.283	−6.365	−6.365	−50.282	−8.432	−58.714	8.375	−0.7	−67.369
24	ZINC69875817	−6.338	−6.344	−6.344	−42.94	−9.309	−52.249	6.364	−0.744	−66.646
25	ZINC78773873	−6.245	−6.245	−6.245	−36.891	−6.359	−43.25	2.04	−0.228	−60.918
26	ZINC83979447	−6.228	−6.228	−6.228	−37.729	−10.974	−48.704	3.42	−0.35	−59.736
27	ZINC19085672	−6.209	−6.209	−6.209	−50.482	−1.848	−52.33	23.644	−0.224	−58.207
28	ZINC40307848	−6.201	−6.206	−6.206	−47.316	−8.567	−55.883	7.962	−0.854	−57.243
29	ZINC06801372	−6.174	−6.174	−6.174	−47.261	−8.178	−55.44	4.873	−1.25	−56.773

Kcal/mol, and (−58.207) Kcal/mol binding energy (ΔG bind) values. When a rigorous examination on binding residues was performed, it was observed that although the three top selected ligands (ZINC 24855054, ZINC58171263, and ZINC08000072) have the lowest binding energy than reference ligand, the binding residues are different. The ZINC 24855054 ligand was perfectly lodged in the binding pocket making Hydrogen bond interaction with SER217, SER276, and Gly275 key residues and shown in (Figs 6 and 7). The obtained docking results justify that ZINC24855054 has better binding stability than the ZINC58171263 and ZINC08000072 ligand in the same binding pocket. So, the binding mode stability of the ZINC24855054, ZINC58171263, and ZINC08000072 ligands on the CpIMPDH active site is further validated by performing an MD run.

Molecular dynamics simulations

MD simulation analysis of docked complexes offers a valuable insight into the thermodynamic and dynamic stability of the biological system. The conformational changes of ligands and protein complex on time scales provide dynamic behavior analysis. Thus, the best-docked pose of top 3 ligands (ZINC24855054,ZINC58171263, and ZINC08000072) along with reference docked complex (CpIMPDH-4IXH) with lowest binding free energy in the CpIMPDH binding site were subjected to 100 nanoseconds (ns) MD study to validate the stability of the proposed intermolecular interactions of the ligand and active site residues during a time frame. The MD analysis data was represented in root mean square deviations (RMSD) and root-mean-square fluctuations (RMSF) plots from the trajectories. The RMSD graph was generated for all backbone atoms and ligands. The RMSF graph was generated for individual amino acid residues. The RMSD value represents the average distance between the backbone atom of receptor protein when interacting with the ligand. The RMSF value measures the average deviation of each receptor protein's residue during the interaction with the ligand. The RMSD and RMSF analysis results for each complex are shown in (Figs 8 and 9), respectively. The RMSD fluctuations of all four complexes, as seen in (Fig. 8), attainedthe equilibrium

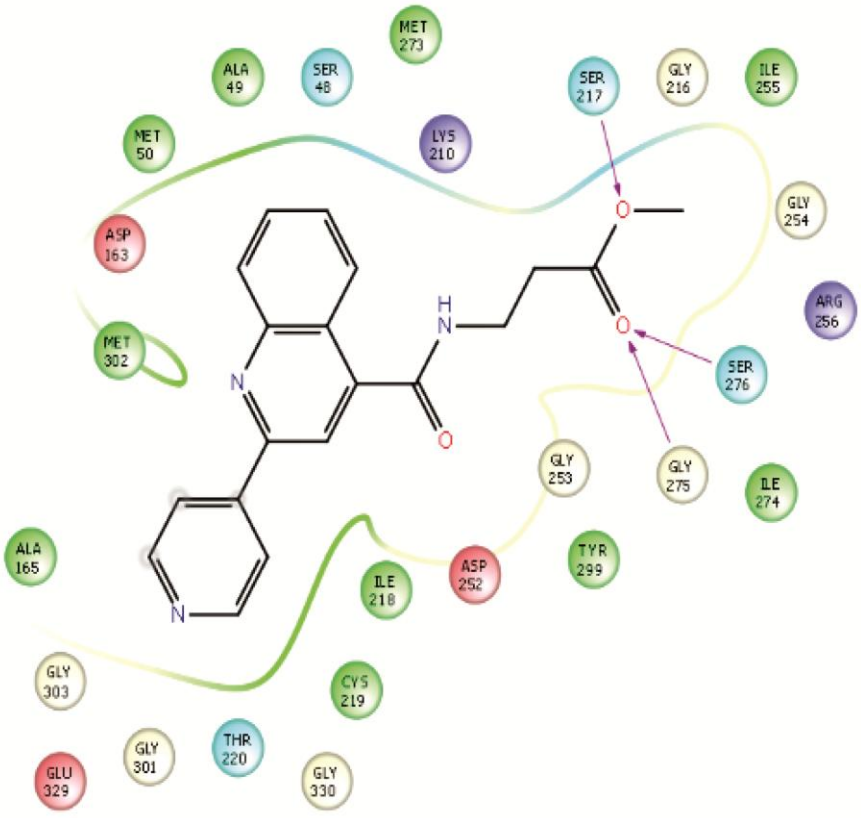

Fig. 6 — The representation of the 2D interaction diagram of the ZINC24855054 ligand with the critical amino acid residues in the CpIMPDH binding pockets

position and remained stable throughout the simulation period where 4IXH-ZINC24855054 complex attained the stable state early on within 10 ns of the timescale. In these protein-ligand complexes, the RMSF values from the trajectories (Fig. 9) show that residual backbone fluctuations were not much different from each other at various residues of the native protein (4IXH) except at the terminal residues and regions mapped by the residues 90-120 and 310-330 which showed significant fluctuations. The observed dynamic stability of the simulated complex reinforced the reliability of the docking results and supported the compound behavior as CpIMPDH inhibitors. As concluded from these studies, shape-based screening (SBS) using known active ligands identified ligands (ZINC24855054, ZINC58171263, and ZINC08000072) having new scaffolds with good binding energies and binding poses. One limitation of this work is that all analysis was performed in *in silico* mode, but a key strength of this research lies in its design and methods for screening new potent ligands.

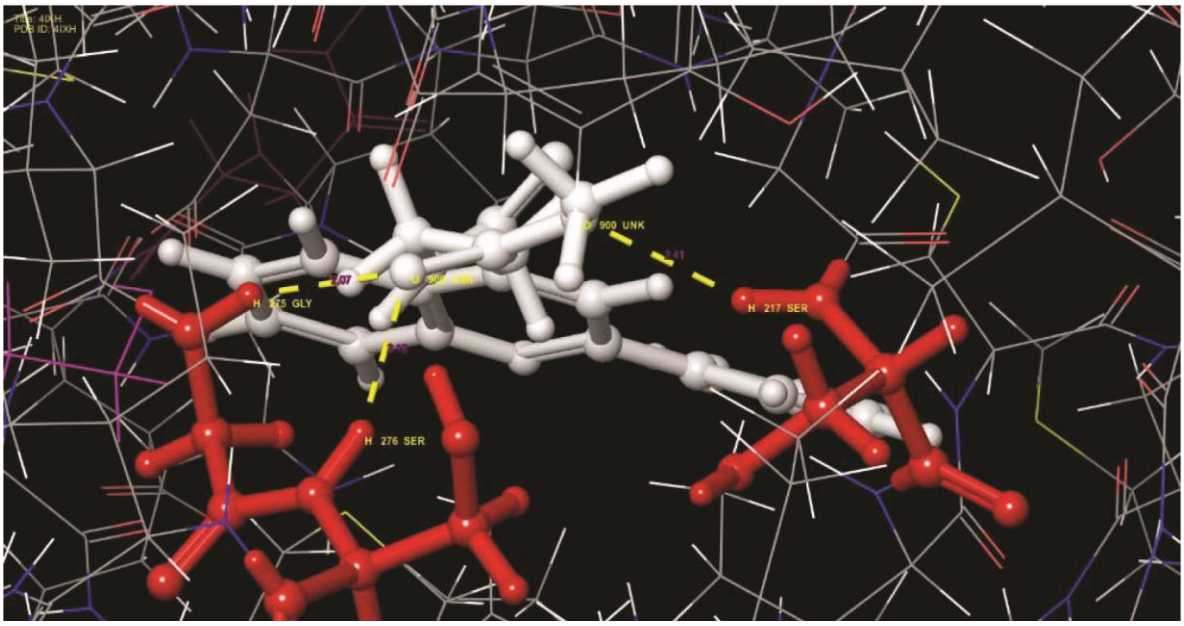

Fig. 7 — Detailed view of ZINC24855054 ligand interaction within CpIMPDH binding pocket

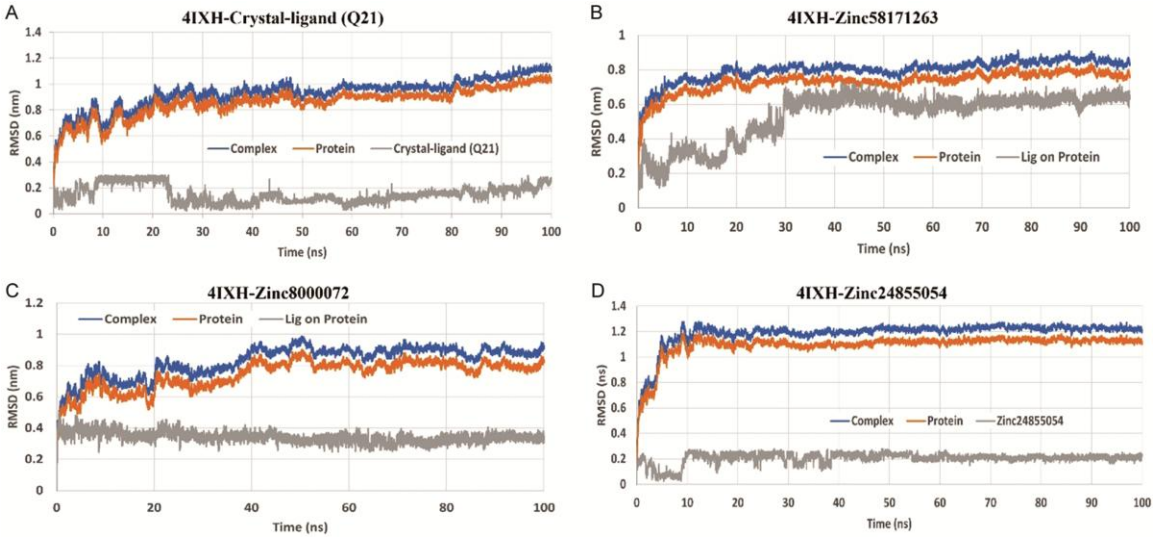

Fig. 8 — Backbone RMSD plot of free and bound form of CpIMPDH complexed with (A) reference ligand Q21; (B) ZINC58171263; (C) ZINC08000072; and (D) ZINC24855054

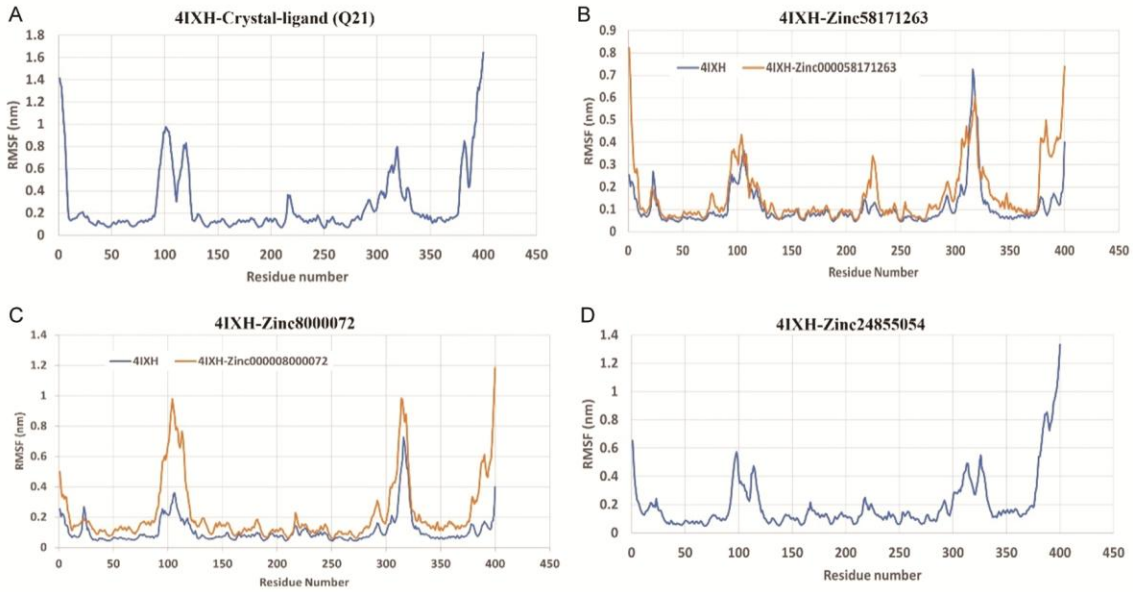

Fig. 9— Backbone RMSF plot of CpIMPDH complexed with (A) reference ligand Q21; (B) ZINC58171263; (C)ZINC08000072; and (D) ZINC24855054

Table 2 — Interaction profile of ligand (ZINC24855054)with receptor protein and interacting amino acids and bond length

Ligand (ZINC24855054) part	Protein (PDB ID:4IXH) Part		Bond Length (Ångström)
Ligand Atom	Atom	Amino acid	
O	H	GLY 275	2.07
O	H	SER 276	2.18
O	H	SER 217	2.14

Conclusion

This study carried out an integrated shape-basedand structure-based virtual screening, ADME analysis, molecular docking, and molecular dynamics studies to identify potent novel small-molecule inhibitors of IMPDH of *C. parvum*.

Cryptosporidium parvum IMPDH (PDB ID: 4IXH) protein was selected as a receptor template. The target protein was prepared by the protein preparation wizard, and the receptor grid was generated by Glide Module. Initially, the Q21 ((2S)-2-(naphthalene-1-yloxy)-N-[2-(pyridine-4-yl)-1,3-benzoxazol-5-yl] propanamide) was docked into the prepared receptor protein for binding mode analysis. In this respect, computational evaluation of a library of 10,000 compounds attained by the similarity search approach deploying previously reported 18ligands against CpIMPDH in a stepwise manner. About 1595 Ligands molecules were prepared by the LigPrep module.In successive steps, 2083 ligands were generated, and ADMET analysis of these ligands was performed by the QikProp module, and Lipinski's rules were applied for all ligands to filter it. Only 1999 ligands were passed Lipinski's rules. These strained ligands from SBS analysis possess a similar functional group as carried by previously identified ligands but possess different scaffolds. All 1999 ligands were docked with the receptor (PDB ID:4IXH)protein by using the Glide High-Throughput Virtual Screening(HTVS) docking method. After this docking, 50%, the best compounds (999 compounds) were processed for the next steps. The HTVS selected ligands were docked with 4IXH protein by using Glide Standard Precision (SP) docking method (47-48). After this docking, 30% best compounds (299 compounds) were processed for the next steps. The SP-selected Ligands were docked with 4IXH protein by using Glide Extra Precision (XP) docking method. After docking, 10%, best compounds (29 compounds) were processed for further analysis. The 29 principal compounds docking results were further processed based on the lowest Glide Score values and the desirable interaction pattern with the key amino acid residues of the CpIMPDH active site obtained from QPLD calculations (Table 2).The effectiveness of docking molecules estimation is considered of vital importance in the availability of a variety of virtual screening ligand complexes. All three protein-ligand complexes' binding free energy was calculated by the Prime/MM-GBSA module. Approximately −80.944 Kcal/mol is the binding free energy of the 4IXH - ZINC24855054 complex. CpIMPDH-ZINC24855054

complex interaction profiles were analyzed, and stability was evaluated using molecular dynamics simulation studies.

On this basis, the top three ligands binding free energy values were computed using Prime/MM-GBSA simulations. The above-discussed filtering approach resulted in three small lead molecules. These small molecules displayed satisfactory ADMET Properties, binding and thermodynamic stability in the complex stage compared with the reference molecule. Among these three ligands, the ZINC24855054 ligand has maximum binding interaction with the active-site residue of the receptor protein. This ligand carries one pyridine ring and one quinolone ring scaffold required for the binding of CpIMPDH. The best-docked pose of ZINC24855054, ZINC58171263, and ZINC08000072 remained stable in the 100ns MD run. The RMSD and RMSF values obtained during MD simulations were also permissible. In view of all these examinations, the experimental exploration of these compounds as anti-CpIMPDH molecules will enable to dispensing of explicit indications for the design and development of CpIMPDH inhibitor molecules with an improved pharmacological outline.

Acknowledgement

I acknowledge and extend my thanks to Dr. Ambedkar Institute of Technology for Handicapped for support to conduct this work smoothly. The authors acknowledge HPC facility of IIT, Delhi for providing computational resources and also the authors would like to thank Prof. Tapan K. Chaudhuri for his insightful suggestions for the work.

Conflict of interest

All authors declare no conflict of interest.

References

1 Hillyer JF, Parasites and parasitology in this SARS-CoV-2, COVID-19 world: An American Society of Parasitologists presidential address. *J Parasitol*, 106 (2020) 859.

2 Bhalchandra S, Cardenas D & Ward HD, Recent breakthroughs and ongoing limitations in *Cryptosporidium* research. *F1000 Res*, (2018).

3 Liu A, Gong B, Liu X, Shen Y, Wu Y, Zhang W & Cao J, A retrospective epidemiological analysis of human *Cryptosporidium* infection in China during the past three decades (1987-2018). *PLoS Negl Trop Dis*, 14 (2020) e0008146.

4 Ahmadpour E, Safarpour H, Xiao L, Zarean M, Hatam-Nahavandi K, Barac A, Picot S, Rahimi MT, Rubino S & Mahami-Oskouei M, Cryptosporidiosis in HIV-positive patients and related risk factors: A systematic review and meta-analysis. *Parasite*, 27 (2020).

5 Madadi S, Mahami-Oskouei M, Rafeey M, Spotin A, Aminisani N, Mahami-Oskouei L, Ghoyounchi R & Berahmat R, Comparative evaluation of *Cryptosporidium* infection in malnourished and well-nourished children: parasitic infections are affected by the interaction of nutritional status and socio-demographic characteristics. *Comp Immunol Microbiol Infect Dis*, 68 (2020) 101406.

6 Tandel J, English ED, Sateriale A, Gullicksrud JA, Beiting DP, Sullivan MC, Pinkston B & Striepen B, Life cycle progression and sexual development of the apicomplexan parasite *Cryptosporidium parvum*. *Nat Microbiol*, 4 (2019) 2226.

7 Arias-Agudelo LM, Garcia-Montoya G, Cabarcas F, Galvan-Diaz AL & Alzate JF, Comparative genomic analysis of the principal *Cryptosporidium* species that infect humans. *Peer J*, 8 (2020) e10478.

8 Bamaiyi PH & Redhuan NEM, Prevalence and risk factors for cryptosporidiosis: A global, emerging, neglected zoonosis. *Asian Biomed*, 10 (2016) 309.

9 Swapna LS & Parkinson J, Genomics of apicomplexan parasites. *Crit Rev Biochem Mol Biol*, 52 (2017) 254.

10 Ryan U & Hijjawi N, New developments in *Cryptosporidium* research. *Int J Parasitol* 45 (2015) 367.

11 Vinayak S, Pawlowic MC, Sateriale A, Brooks CF, Studstill CJ, Bar-Peled Y, Cipriano MJ & Striepen B, Genetic modification of the diarrhoeal pathogen *Cryptosporidium parvum*. *Nature*, 523 (2015) 477.

12 Branda S, Courtney CM, Sinha A, Poorey K, Schoeniger JS, LaBauve AE & Williams KP, Elucidation & manipulation of host-pathogen interactions for development of countermeasures against intracellular bacterial pathogen Burkholderiapseudomallei. (2018).

13 Beverley SM, CRISPR for *Cryptosporidium*. *Nature*, 523 (2015) 413.

14 Mukerjee A, Iyidogan P, Castellanos-Gonzalez A, Cisneros JA, Czyzyk D, Ranjan AP, Jorgensen WL, White AC, Vishwanatha JK & Anderson KS, A nanotherapy strategy significantly enhances anticryptosporidial activity of an inhibitor of bifunctional thymidylate synthase-dihydrofolate reductase from *Cryptosporidium*. *Bioorg Med Chem Lett*, 25 (2015) 2065.

15 Cabada MM & White AC, Treatment of cryptosporidiosis: Do we know what we think we know? *Curr Opin Infect Dis*, 23 (2010) 494.

16 Manjunatha UH, Chao AT, Leong FJ & Diagana TT, Cryptosporidiosis Drug Discovery: Opportunities and Challenges. *ACS Infect Dis*, 2 (2016) 530.

17 Li RJ, Wang YL, Wang QH, Huang WX, Wang J & Cheng MS, Binding mode of inhibitors and *Cryptosporidium parvum* IMP dehydrogenase: A combined ligand- and receptor-based study. *SAR QSAR Environ Res*, 26 (2015) 421.

18 Gollapalli DR, MacPherson IS, Liechti G, Gorla SK, Goldberg JB & Hedstrom L, Structural determinants of inhibitor selectivity in prokaryotic IMP dehydrogenases. *Chem Biol*, 17 (2010) 1084.

19 Hedstrom L, Liechti G, Goldberg JB & Gollapalli DR, The Antibiotic Potential of Prokaryotic IMP Dehydrogenase Inhibitors. *Curr Med Chem*, 18 (2011) 1909.

20 Leelananda SP & Lindert S, Computational methods in drug discovery. *Beilstein J Org Chem*, 12 (2016) 2694.

21 Ferreira LG, Dos Santos RN, Oliva G & Andricopulo AD, Molecular docking and structure-based drug design strategies. *Molecules*, 20 (2015) 13384.

22 Choudhury M, Sharma D, Das M & Dutta K, Molecular docking studies of natural and synthetic compounds against human secretory PLA2 in therapeutic intervention of inflammatory diseases and analysis of their pharmacokinetic properties. *Indian J Biochem Biophys*, 59 (2022) 33.

23 Liu X, Shi D, Zhou S, Liu H, Liu H & Yao X, Molecular dynamics simulations and novel drug discovery. *Expert Opin Drug Discov*, 13 (2018) 23.

24 Toppo AL, Yadav M, Dhagat S, Ayothiraman S & Jujjavarapu SE, Molecular docking and ADMET analysis of synthetic statins for HMG-CoA reductase inhibition activity. *Indian J Biochem Biophys*, 58 (2021) 127.

25 De Vivo M, Masetti M, Bottegoni G & Cavalli A, Role of molecular dynamics and related methods in drug discovery. *J Med Chem*, 59 (2016) 4035.

26 Sastry GM, Dixon SL & Sherman W, Rapid shape-based ligand alignment and virtual screening method based on atom/feature-pair similarities and volume overlap scoring. *J Chem Inf Model*, 51 (2011) 2455.

27 Gimeno A, Ojeda-Montes MJ, Tomás-Hernández S, Cereto-Massagué A, Beltrán-Debón R, Mulero M, Pujadas G & Garcia-Vallvé S, The Light and Dark Sides of Virtual Screening: What Is There to Know? *Int J Mol Sci*, 20 (2019) 1375.

28 Bao G, Zhou L, Wang T, He L & Liu T, A Combined Pharmacophore-Based Virtual Screening, Docking Study and Molecular Dynamics (MD) Simulation Approach to Identify Inhibitors with Novel Scaffolds for Myeloid cell leukemia (Mcl-1). *Bull Korean Chem Soc*, 35 (2014) 2097.

29 Sterling T & Irwin JJ, ZINC 15 - Ligand Discovery for Everyone. *J Chem Inf Model*, 55 (2015) 2324.

30 Schrodinger LLC, Schrodinger Suite 2012 Protein Preparation Wizard; Epik verstion 2.3, Impact version 5.8, Prime vesion 3.1. *(New York Schrodinger)*, 2012.

31 Ioakimidis L, Thoukydidis L, Mirza A, Naeem S & Reynisson J, Benchmarking the reliability of QikProp. Correlation between experimental and predicted values. *QSAR Comb Sci*, 27 (2008) 445.

32 Striepen B, White MW, Li C, Guerini MN, Malik S-B, Logsdon JM, Liu C & Abrahamsen MS, Genetic complementation in apicomplexan parasites. *Proc Natl Acad Sci U S A*, 99 (2002) 6304.

33 Kim Y, Maltseva N, Mulligan R, Makowska-Grzyska M, Gu M & Gollapalli D, Crystal Structure of the Catalytic Domain of the Inosine Monophosphate Dehydrogenase from Bacillus anthracis in the complex with IMP and the inhibitor P200. (2017).

34 Laskowski RA, Rullmann JAC, MacArthur MW, Kaptein R & Thornton JM, AQUA and PROCHECK-NMR: programs for checking the quality of protein structures solved by NMR. *J Biomol NMR*, 8 (1996) 477.

35 Harder E, Damm W, Maple J, Wu C, Reboul M, Xiang JY, Wang L, Lupyan D, Dahlgren MK & Knight JL, OPLS3: A force field providing broad coverage of drug-like small molecules and proteins. *J Chem Theory Comput*, 12 (2016) 281.

36 Halgren TA, Murphy RB, Friesner RA, Beard HS, Frye LL, Pollard WT & Banks JL, Glide: A new approach for rapid, accurate docking and scoring. 2. Enrichment factors in database screening. *J Med Chem*, 47 (2004) 1750.

37 Friesner RA, Murphy RB, Repasky MP, Frye LL, Greenwood JR, Halgren TA, Sanschagrin PC & Mainz DT, Extra precision glide: Docking and scoring incorporating a model of hydrophobic enclosure for protein−ligand complexes. *J Med Chem*, 49 (2006) 6177.

38 Cho AE, Guallar V, Berne BJ & Friesner R, Importance of accurate charges in molecular docking: quantum mechanical/molecular mechanical (QM/MM) approach. *J Comput Chem*, 26 (2005) 915.

39 Bochevarov AD, Watson MA, Greenwood JR & Philipp DM, Multiconformation, density functional theory-based p K a prediction in application to large, flexible organic molecules with diverse functional groups. *J Chem Theory Comput*, 12 (2016) 6001.

40 Yu HS, Watson MA & Bochevarov AD, Weighted Averaging Scheme and Local Atomic Descriptor for p K a Prediction Based on Density Functional Theory. *J Chem Inf Model*, 58 (2018) 271.

41 Genheden S & Ryde U, The MM/PBSA and MM/GBSA methods to estimate ligand-binding affinities. *Expert Opin Drug Discov*, 10 (2015) 449.

42 Sirous H, Chemi G, Campiani G & Brogi S, An integrated in silico screening strategy for identifying promising disruptors of p53-MDM2 interaction. *Comput Biol Chem*, 83 (2019) 107105.

43 Kumari R, Kumar R, Consortium OSDD & Lynn A, g_mmpbsa–A GROMACS tool for high-throughput MM-PBSA calculations. *J Chem Inf Model*, 54 (2014) 1951.

44 Lindahl E, Bjelkmar P, Larsson P, Cuendet MA & Hess B, Implementation of the charmm force field in GROMACS: Analysis of protein stability effects from correction maps, virtual interaction sites, and water models. *J Chem Theory Comput*, 6 (2010) 459.

45 Bernardi A, Faller R, Reith D & Kirschner KN, ACPYPE update for nonuniform 1–4 scale factors: Conversion of the GLYCAM06 force field from AMBER to GROMACS. *Software X*, 10 (2019) 100241.

46 Huston CD, Spangenberg T, Burrows J, Willis P, Wells TNC & van Voorhis W, A proposed target product profile and developmental cascade for new cryptosporidiosis treatments. *PLoS Negl Trop Dis*, (2015).

47 Kirubakaran S, Gorla SK, Sharling L, Zhang M, Liu X, Ray SS, MacPherson IS, Striepen B, Hedstrom L & Cuny GD, Structure-activity relationship study of selective benzimidazole-based inhibitors of *Cryptosporidium parvum* IMPDH. *Bioorganic Med Chem Lett*, (2012).